On the Complexation of Ferric Ions by Reduced Nicotinamide Adenine Dinucleotide†

Menachem Gutman* and Michael Eisenbach

ABSTRACT: In acid aqueous solutions, ferric ions and NADH were found to react rapidly to form a blue charge-transfer complex with a stoichiometry of $Fe^{3+}(NADH)_2$. This complex is unstable and decomposes in a redox reaction with Fe^{2+} and NAD^+ as products. The formation of the complex was studied under similar conditions by the stopped-flow technique and found to be a two-step reaction (see eq 1 and 2 of text). The rate constants of these two reactions were calculated from both kinetics and equilibrium studies. Within experimental error the results obtained by the two methods were the same ($k_1 = (5.0 \pm 0.2) \times 10^3$ M^{-1} sec^{-1}, $k_{-1} = 0.6 \pm 0.1$ sec^{-1}; $k_2 = (1.30 \pm 0.05) \times 10^3$ M^{-1} sec^{-1}, $k_{-2} = 0.03 \pm 0.01$ sec^{-1}). The relatively small magnitude of k_{-2} is the explanation for the complete conversion of Fe^{3+} into the $Fe^{3+}(NADH)_2$ complex. The two complexes have similar absorption spectra with a maximum at 540 nm, except that the extinction coefficient of the $Fe^{3+}(NADH)$ is lower than that of $Fe^{3+}(NADH)_2$. The properties of the $Fe^{3+}(NADH)$ complex are discussed.

The oxidation of NADH[1] by ferric ions is a complex reaction that can be divided into three main steps: the formation of the reactive complex, the one-electron oxidation of NADH by the ferric ion and the resulting decomposition of the complex and, finally, the reaction between the oxidation products of the NADH. The last two steps in these reactions were reported before (Gutman *et al.*, 1968). In this study, the formation of the $Fe^{3+}(NADH)_2$ complex is described.

Under the chosen experimental conditions, the formation of $Fe^{3+}(NADH)_2$ is slow enough to be followed by the stopped-flow technique. It was observed that the reaction occurs in two steps where $Fe^{3+}(NADH)$ acts as an intermediate.

The two complexes, $Fe^{3+}(NADH)$ and $Fe^{3+}(NADH)_2$, are very similar in their spectral properties: both have an absorption maximum at the same wavelength and their extinction coefficients are of comparable magnitudes. As a result, the kinetic analysis had to be carried simultaneously for the two complexes. First, the macroscopic rate constants were determined and from them, the forward and backward microscopic rate constants were computed.

Materials and Methods

The NADH (Sigma) was dissolved in 0.001 M $NaHCO_3$ (pH 7.8) and its concentration was determined spectrophotometrically; $Fe(ClO_4)_3$ (Fluka A. G.) was dissolved in 0.2 M glycine (pH 2.0) and its concentration was determined with 1,10-phenantroline (Merck) (Massey, 1957). Spectrophotometric measurements of short times were carried out with a Durrum-Gibson stopped-flow spectrophotometer at 25°. The optical path length in the cuvet was 2 cm. The reaction was followed at 540 nm with a slit width of 0.07 mm, equivalent to a half-bandwidth of 0.2 nm. The tracing was projected on a storage oscilloscope with sweeping times of 1–2000 msec/division and photographed, and the data were extracted manually. All the computations and plots were performed by a C.D.C. 6000 computer.

Results and Discussion

In choosing the conditions for the experiments, the opposing effect of pH had to be considered. Low pH favors the formation of the complex, but it leads to acid decomposition of NADH (Johnston *et al.*, 1963; Kaplan, 1960; Burton and Kaplan, 1963; Gutman *et al.*, 1968). When studying the redox reaction of the complex, the pH was kept at 3.5, thus slowing the acid decomposition of NADH with respect to the redox reaction (Gutman *et al.*, 1968). In this study, the reactions were fast enough so that the acid decomposition could be neglected, and to ensure maximal formation of the complex, the pH was lowered to 2.0.

The results of a typical kinetic experiment are shown in Figure 1. The changes in absorbance can be divided into three phases: in the initial phase there is a rapid increase in absorbance, slowing down to the second phase and finally, a very slow decrease in absorbance as seen after the arrow marking on line C (Figure 1). The first two phases are associated with the formation of the complex, while the latter is the redox reaction within the complex (Gutman *et al.*, 1968).

Calculation of the Macroscopic Rate Constants. With NADH concentration 20 times higher than that of the ferric ions, we assumed that its concentration was constant, and treated the reaction as following psuedo-first-order kinetics.

Figure 2 is the logarithmic plot of absorbance changes with respect to time, and the linearity is in accord with the first order dependence on the iron concentration. There are two phases in the formation of the complex which are compatible with the mechanism

$$Fe^{3+} + NADH \underset{k_{-1}}{\overset{k_1}{\rightleftharpoons}} Fe^{3+}(NADH) \quad (1)$$

$$Fe^{3+}(NADH) + NADH \underset{k_{-2}}{\overset{k_2}{\rightleftharpoons}} Fe^{3+}(NADH)_2 \quad (2)$$

where in the first phase $Fe^{3+}(NADH)$ is formed, followed by the appearance of $Fe^{3+}(NADH)_2$. This mechanism will be

† From the Department of Biochemistry, George S. Wise Center for Life Sciences, Faculty of Life Sciences, Tel-Aviv University, Ramat-Aviv, Tel-Aviv, Israel. *Received December 12, 1972.*

[1] Abbreviations used are: NADH and NAD^+, nicotinamide adenine dinucleotide, the reduced and oxidized forms, respectively.

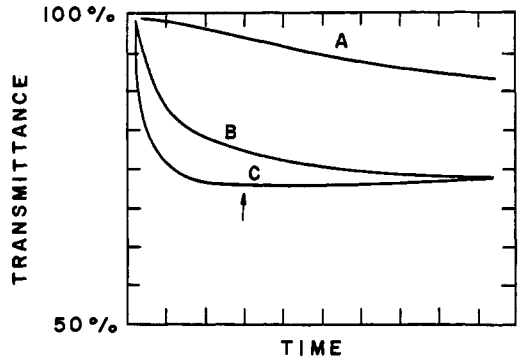

FIGURE 1: The variation of transmittance with time after mixing of 0.2 ml of 0.1435 mM $Fe(ClO_4)_3$ in 0.2 M glycine (pH 2.0) with 0.2 ml of 2.78 mM NADH in 1 mM $NaHCO_3$ in a Durrum-Gibson stopped-flow spectrophotometer. The reaction was monitored at 540 nm with a slit width of 0.07 mm at 25.0°. The time scale is: (A) 0.01, (B) 0.2, (C) 1 sec per division.

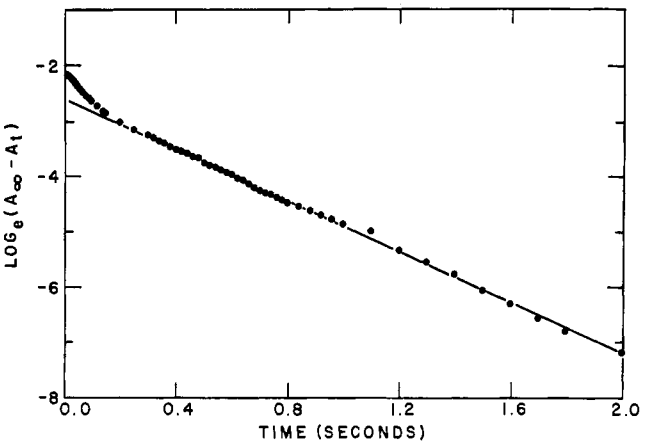

FIGURE 2: Variation of ln $(A_\infty - A_t)$ with time. The points were extracted from an experiment, identical with that shown in Figure 1, only that the NADH concentration was raised to 4.18 mM.

used for the analysis of the experimental data. It was once suggested (Gutman *et al.*, 1968) that $Fe^{3+}(NADH)_3$ might also exist, but a detailed analysis of titration curves indicated later that $Fe^{3+}(NADH)_2$ is the final product (M. Gutman, unpublished results).

In order to obtain the absorption spectrum of the Fe^{3+}-(NADH) complex, we mixed Fe^{3+} and NADH at a ratio of 1:1 and measured the absorbance after 25 msec. Under these conditions the $Fe^{3+}(NADH)$ would be the dominant species. The absorption spectrum obtained by running the kinetics at different wavelengths was very similar to that of Fe^{3+}-$(NADH)_2$ (Gutman *et al.*, 1968). As we were unable to use a wavelength where only one species is absorbing, we carried the kinetic analysis at 540 nm, where both of them have maximal absorbance.

The linearity of the line after 250 msec (Figure 2) suggests that under these conditions only one reaction is observed (eq 2), and the macroscopic rate constant (m_2) (Fleck, 1971) for this reaction was calculated from the slope and is given in Table I. The other macroscopic rate constant (m_1) was more difficult to derive, as even at very short times the logarithmic plot is not straight enough for its determination. To be able to evaluate m_1, we treated $Fe^{3+}(NADH)$ as an intermediate in the formation of $Fe^{3+}(NADH)_2$. As there is no direct method to follow the concentration of the intermediate complex, we went through the following approach. We assumed hypothetical conditions where the reaction goes in two steps. The first one is an instantaneous formation of $Fe^{3+}(NADH)$ without affecting the absorbance at 540 nm ($\epsilon_1 = 0$). The second step is the appearance of $Fe^{3+}(NADH)_2$ with the measured rate constant m_2 and the extinction coefficient (ϵ_2). In such formation the appearance of the absorbance at 540 nm is according to

$$A = A_\infty(1 - e^{-m_2 t}) \tag{3}$$

This equation is depicted as the straight line in Figure 3. The deviation of the experimental line from this hypothetical line is due to the fact that $Fe^{3+}(NADH)$ is formed at a finite rate and associated with an increase in the absorbance at 540 nm ($\epsilon_1 > 0$).

The difference between the two lines in Figure 3, which we define as Y, is a function related to the appearance and disappearance of the intermediate $Fe^{3+}(NADH)$. The Y function is zero, both at $t = 0$ and $t \to \infty$; thus it goes through a maximum. The time at which it attains its maximal value (t_{max}) can be used to evaluate m_1.

The value of Y at any given time is

$$Y = A_t - A_\infty(1 - e^{-m_2 t}) \tag{4}$$

where A_t is the observed absorbance at time t. A_t can also be expressed as the sum of the absorbances of both $Fe^{3+}(NADH)$ and $Fe^{3+}(NADH)_2$

$$A_t = \epsilon_1[Fe^{3+}(NADH)] + \epsilon_2[Fe^{3+}(NADH)_2] \tag{5}$$

The concentration of $Fe^{3+}(NADH)$ and $Fe^{3+}(NADH)_2$ could be obtained from the equations of Lowry and John (1910) for sequential, reversible first-order reactions. As will be documented later, we could simplify these equations by assuming that k_{-2} is negligible with respect to the other kinetic constants and can be eliminated from the kinetic equations. Under these conditions, the Lowry and John equations will take the form

$$[Fe^{3+}] = [Fe^{3+}]_0\left(\frac{m_1 - k_1'}{m_1 - m_2}e^{-m_2 t} + \frac{k_1' - m_2}{m_1 - m_2}e^{-m_1 t}\right) \tag{6}$$

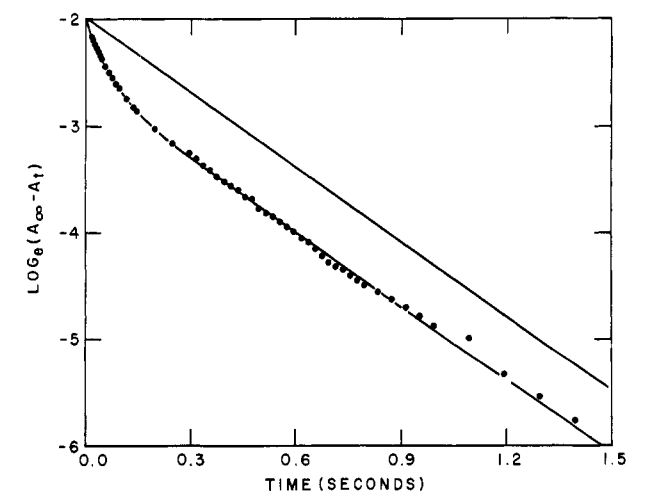

FIGURE 3: Data from Figure 2 in expanded scales. The straight line represents kinetic behavior under the hypothetical conditions as explained in the text.

TABLE I:[a] Macroscopic and Microscopic Rate Constants for the Formation of Fe^{3+}(NADH) and $Fe^{3+}(NADH)_2$.

[NADH] (mM)	m_2 (sec^{-1})	m_1 (sec^{-1})	t_{max} (msec)	k_1 (M^{-1} sec^{-1})	k_1' (sec^{-1})	k_2 (M^{-1} sec^{-1})	k_2' (sec^{-1})	k_{-1} (sec^{-1})
2.09	2.43	11.4 ± 0.3	170 ± 5	(5.0 ± 0.2) × 10^3	10.4 ± 0.4	(1.30 ± 0.05) × 10^3	2.7 ± 0.1	0.6 ± 0.1
1.39	1.71	7.7 ± 0.2	255 ± 10	(5.0 ± 0.2) × 10^3	7.0 ± 0.3	(1.30 ± 0.05) × 10^3	1.8 ± 0.1	0.6 ± 0.1

[a] The rate constants are calculated from kinetic studies with Fe^{3+} (0.072 mM) in 0.1 M glycine buffer (pH 2.0) at 25°. The NADH concentration is given in the table.

$$[Fe^{3+}(NADH)] = [Fe^{3+}]_0 \frac{k_1'}{m_1 - m_2}(e^{-m_2 t} - e^{-m_1 t}) \quad (7)$$

$$[Fe^{3+}(NADH)_2] = [Fe^{3+}]_0\left(1 - \frac{m_1}{m_1 - m_2}e^{-m_2 t} + \frac{m_2}{m_1 - m_2}e^{-m_1 t}\right) \quad (8)$$

where $k_1' = k_1[NADH]_0$. Substituting eq 7 and 8 into eq 5, and this into eq 4, gives the final expression for the Y function

$$Y = [Fe^{3+}]_0 \times \left(\frac{\epsilon_1 k_1' - \epsilon_2 m_1}{m_1 - m_2}e^{-m_2 t} + \frac{\epsilon_2 m_2 - \epsilon_1 k_1'}{m_1 - m_2}e^{-m_1 t} + \epsilon_2 e^{-m_2 t}\right) \quad (9)$$

This function can be shown to have a maximum at

$$t_{max} = \frac{\ln (m_2/m_1)}{m_2 - m_1} \quad (10)$$

Figure 4 is the variation of the Y value, calculated from eq 4, with time. The values of m_2, t_{max}, and the resulting m_1 calculated from eq 10 for two concentrations of NADH are given in Table I.

Determination of the Microscopic Rate Constants. It was shown previously that all the Fe^{3+} ions can be converted to $Fe^{3+}(NADH)_2$ (Gutman *et al.*, 1968). Therefore k_{-2} must be much smaller than k_2 (eq 2). Confirmation of this can be found in the equations of Lowry and John (1910), in which $[Fe^{3+}(NADH)_2]_\infty = [Fe^{3+}]_0$ only when $k_{-2} = 0$.

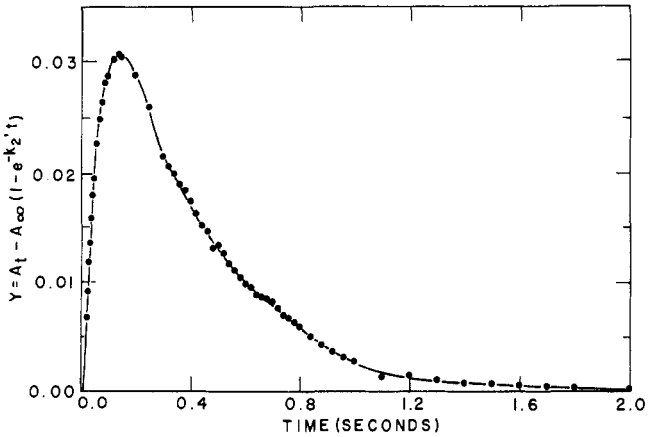

FIGURE 4: The variation of the variable Y with time, as calculated from eq 4. The NADH and ferric ion concentrations are as in Figure 2.

The other microscopic rate constants were calculated from Lowry and John equations in terms of the macroscopic rate constants

$$m_1 + m_2 = k_1' + k_{-1} + k_2' \quad (11)$$

$$m_1 m_2 = k_1' k_2' \quad (12)$$

and are given in Table I. The agreement between the second-order rate constants, calculated for the two NADH concentrations, validates our assumption that the reaction follows pseudo-first-order kinetics. It was felt that using higher NADH concentrations will not yield any new information. Lowering the NADH concentration could only lead to deviation from the pseudo-first-order kinetics.

Determination of the Extinction Coefficients. The extinction coefficient for $Fe^{3+}(NADH)_2$, ϵ_2, was redetermined under the conditions of these experiments and found to be ϵ_2(540 nm) = 875 ± 5 M^{-1} cm^{-1}, essentially the same as reported previously, 900 M^{-1} cm^{-1} (Gutman *et al.*, 1968). The value of ϵ_1 was derived by substituting eq 7 and 8 into eq 5

$$A_t = [Fe^{3+}]_0\left[\frac{\epsilon_1 k_1'}{m_1 - m_2}(e^{-m_2 t} - e^{-m_1 t}) + \epsilon_2\left(1 - \frac{m_1}{m_1 - m_2}e^{-m_2 t} + \frac{m_2}{m_1 - m_2}e^{-m_1 t}\right)\right] \quad (13)$$

As all of the parameters except ϵ_1 are known, ϵ_1 was calculated for the two NADH concentrations for the whole time range. The value of ϵ_1 was found to be $\epsilon_1 = 590 \pm 30$ M^{-1} cm^{-1}.

Figure 5 is a reconstruction of the observed results with the calculated kinetic and absorption parameters. The line was calculated from eq 13, and its fit to the observed absorbancies is evident.

Estimation of the Equilibrium Constants. The equilibrium constants for the formation of the two complexes were determined from a titration curve of Fe^{3+} with NADH. The absorbance at 540 nm can be represented by the following set of equations

$$A_t = \epsilon_1[Fe^{3+}(NADH)] + \epsilon_2[Fe^{3+}(NADH)_2] \quad (5)$$

$$[Fe^{3+}]_0 = [Fe^{3+}] + [Fe^{3+}(NADH)] + [Fe^{3+}(NADH)_2] \quad (14)$$

$$[NADH]_0 = [NADH] + [Fe^{3+}(NADH)] + 2[Fe^{3+}(NADH)_2] \quad (15)$$

$$K_1 = \frac{[Fe^{3+}(NADH)]}{[Fe^{3+}]\,[NADH]} \quad (16)$$

TABLE II:[a] Equilibrium Constants and the Backward Microscopic Rate Constants for the Reaction between Fe^{3+} and NADH.

Parameter	Value
K_1	$(7.3 \pm 2.5) \times 10^3$ M^{-1}
K_2	$(4.0 \pm 1.5) \times 10^4$ M^{-1}
$K_{1,2}$	$(2.9 \pm 1.1) \times 10^8$ M^{-2}
k_{-1}	0.7 ± 0.1 sec^{-1}
k_{-2}	0.03 ± 0.01 sec^{-1}

[a] The results are derived as detailed in the text from titration of Fe^{3+} (0.0029 mM) with NADH in 0.1 M glycine buffer (pH 2.0), 25°.

$$K_2 = \frac{[Fe^{3+}(NADH)_2]}{[Fe^{3+}(NADH)][NADH]} \quad (17)$$

In these five equations we have six variables; thus they cannot be solved directly. As the variables K_1 and K_2 will be constant for any set of NADH and Fe^{3+} concentrations, by solving the equations simultaneously for two NADH concentrations, we obtain a set of ten equations with ten variables. As eq 16 and 17 are nonlinear, the Newton–Raphson approximation method had to be employed. The resulting equilibrium constants, K_1, K_2, and the overall constant ($K_{1,2} = K_1K_2$), are given in Table II. From the equilibrium constants, we also estimated k_{-1} and k_{-2}. The values of k_{-1} derived from the two methods, kinetic and equilibrium studies, are the same within experimental error (0.7 and 0.6 sec^{-1}, respectively). The small value of k_{-2} justifies the approximation $k_{-2} \simeq 0$ used in the kinetic analysis. It is the slow rate of the dissociation of $Fe^{3+}(NADH)_2$ to $Fe^{3+}(NADH)$ which pulls the equilibrium to complete formation of $Fe^{3+}(NADH)_2$ with negligible equilibrium concentrations of $Fe^{3+}(NADH)$.

The similarity of the λ_{max} of the two complexes and the comparable magnitudes of ϵ_1 and ϵ_2, suggest that the same spectral transition occurs in both complexes. The redox reaction occurring in the $Fe^{3+}(NADH)_2$ complex was suggested to be an electron transfer from the ligand (reduced nicotin amide moiety) to the ferric orbitals (Gutman *et al.*, 1968). This redox reaction was enhanced by photoexcitation of the complex (M. Gutman, unpublished results); thus it seems that in the excited state, the electron transfer is followed by the redox reaction. In the $Fe^{3+}(NADH)$ complex, the redox reaction cannot be observed due to the short duration where this complex exists. Yet based on the similarity of the absorption spectra, a redox reaction in the excited $Fe^{3+}(NADH)$ can be expected.

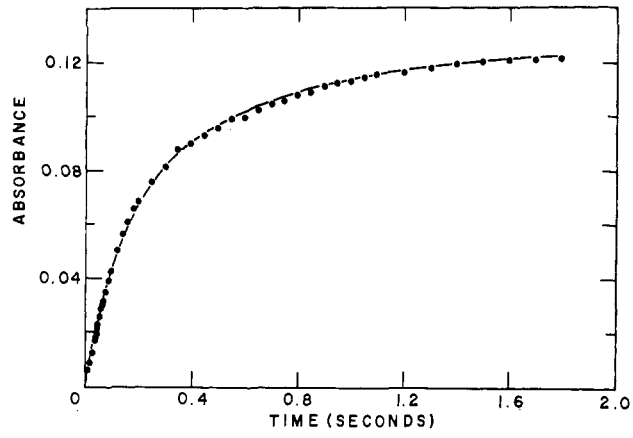

FIGURE 5: Comparison between the observed and the calculated kinetics. The circles represent the experimental data given in Figure 1 and the line was calculated according to eq 13 with $[Fe^{3+}]$ = 0.0718 mM and [NADH] = 1.39 mM. The kinetic constants and extinction coefficients are those given in Table I.

Finally, it is tempting to point out a resemblance between the reaction of the ferric ion with NADH and enzymic oxidation of NADH. The enzymic oxidation of NADH can be divided into three steps: binding of NADH to the active site, its excitation to a more reactive form and, finally, its oxidation by the enzyme. By analogy, we can observe the same steps in this reaction: NADH forms a complex with ferric ion, the complex is excited by a charge transfer and finally an internal redox reaction occurs. Thus the ferric ion can substitute for all three steps expected from the active site. If this analogy is to be further investigated, the $Fe^{3+}(NADH)$ complex is the simpler model. Yet owing to its intermediary nature, it can be the dominant complex only a very short time after mixing. For such future studies, the rate constants given in this publication will be a necessary tool.

References

Burton, R. M., and Kaplan, N. O. (1963), *Arch. Biochem. Biophys 101*, 150.

Fleck, G. M. (1971), Chemical Reaction Mechanisms, New York, N. Y., Holt, Rinehart and Winston, p 76.

Gutman, M., Margalit, R., and Schejter, A. (1968), *Biochemistry 7*, 2778.

Johnston, C. C., Gardner, J. L., Suelter, C. H., and Metzler, D. E. (1963), *Biochemistry 2*, 689.

Kaplan, N. O. (1960), *Enzymes 3*, 105.

Lowry, T. M., and John, W. T. (1910), *J. Chem. Soc. 97*, 2634.

Massey, V. (1957), *J. Biol. Chem. 229*, 763.